A Spatiotemporally Explicit Paleoenvironmental Framework for the Middle Stone Age of Eastern Africa

Lucy Timbrell (lucy.timbrell@liverpool.ac.uk)
University of Liverpool
Matt Grove
University of Liverpool
Andrea Manica
University of Cambridge
Stephen Rucina
National Museums of Kenya
James Blinkhorn (blinkhorn@shh.mpg.de)
Max Planck Institute for the Science of Human History

Research Article

Keywords: Middle Stone Age, eastern Africa, palaeoenvironments, Homo sapiens, paleoclimatic models

Posted Date: September 20th, 2021

DOI: https://doi.org/10.21203/rs.3.rs-879959/v1

Version of Record: A version of this preprint was published at Scientific Reports on March 7th, 2022. See the published version at https://doi.org/10.1038/s41598-022-07742-y.

Abstract

Eastern Africa has played a prominent role in debates about human evolution and dispersal due to the presence of rich archaeological, palaeoanthropological and palaeoenvironmental records. However, substantial disconnects occur between the spatial and temporal resolutions of these data that complicate their integration. Here, we apply high-resolution climatic simulations of two key parameters, mean annual temperature and precipitation, and a biome model, to produce a highly refined characterisation of the environments inhabited during the eastern African Middle Stone Age. Occupations are typically found in sub-humid climates and landscapes dominated by or including tropical xerophytic shrubland. Marked expansions from these core landscapes include movement into hotter, low-altitude landscapes in Marine Isotope Stage 5 and cooler, high-altitude landscapes in Marine Isotope Stage 3, with the recurrent inhabitation of ecotones between open and forested habitats. Through our use of high-resolution climate models, we demonstrate a significant independent relationship between past precipitation and patterns of Middle Stone Age stone tool use overlooked by previous studies. Engagement with these models not only enables spatiotemporally explicit examination of climatic variability across Middle Stone Age assemblages in eastern Africa but enables clearer characterisation of the habitats early human populations were adapted to, and how they changed through time.

1. Introduction

Fossil, archaeological, and environmental records, together with the geographic placement of the region, suggest that eastern Africa played a prominent role in the evolution and dispersal of our species, *Homo sapiens* [1]. The mosaic morphology of recently discovered Mtoto fossils at Panga Ya Saidi demonstrates that eastern Africa sustained great diversity amongst Middle Stone Age (MSA) populations into the Late Pleistocene [2], supporting a pan-African origin for *H. sapiens* rather than a single centre of endemism [3,4]. Across the continent, the MSA is becoming increasingly associated with the emergence of our species due to the near-simultaneous appearance of cultural innovations diagnostic of the MSA and hominin fossils possessing ‘modern’ features autapomorphic to *H. sapiens* [5–8]. The MSA archaeology record in eastern Africa is particularly rich compared to other regions, largely because of an extensive research history combining extensive use of chronometric dating and controlled excavation as well as its ideal conditions for preservation. This makes it an essential testing ground for hypotheses regarding modern human behavioural evolution [9–13], especially in relation to palaeoclimatic change [14–17].

Historically, there have been relatively scarce terrestrial climate records from eastern Africa, particularly in contrast to the richness of the archaeological record [18]. Over the past decade, recently assembled lacustrine records now provide evidence for climatic changes in several major basins spanning the region. The near-continuous core record from Lake Tana demonstrates increased climatic fluctuation towards the end of the penultimate glacial period, followed by abrupt change to stable humid conditions during Marine Isotope Stage (MIS) 5e-c [19]. The Lake Tana record, from which Ca/Ti elemental ratios are used as a proxy for effective moisture, has been used to assess Out of Africa dispersal chronologies [15]. However, the lack of stratigraphically secure archaeological records proximate to the core site limits the

potential to make strong links between dispersals and climate change. Elsewhere, at Olorgesailie high-resolution core data is associated with Acheulean and MSA deposits just 24km away from the drill site, allowing for the identification of a period of increased variability coinciding with the origin of the MSA [20, 21]. This is supported by the pollen records at nearby Lake Magadi where the general trend of increased aridification for this period is also reported [22]. Late Pleistocene records from the Chew Bahir basin similarly demonstrate a series of wet-dry transitions of varying amplitude and duration through K counts [23], with the early modern human fossil site Omo Kibish lying close to (but not within) the basin. This record therefore could potentially offer a climatic context for MSA occupations of the site, considering that highly favourable humid conditions are reported at 200 – 125,000 years ago (ka) [23] which broadly corresponds to the new date of the Omo fossils of 212 ± 16 ka [24]. Despite this improvement in resolution, paleoclimatic patterns and the records used to generate them are diverse (demonstrated in Fig. 1) and rooted in a small number of lake basins, complicating their use with the widely distributed MSA records in the region.

Archaeological studies of the eastern African MSA have noted a link between the distribution of sites, behavioural diversity, and environmental conditions [9–13]. Basell [9] made a key contribution by integrating modelled ecological data with a landmark synthesis of MSA assemblages. This highlighted the placement of MSA site locations near to but not necessarily within wooded ecologies, stressing the importance of ecotonal settings for enduring habitability in the region. Tryon and Faith [13] made important advances in the quantitative assessment of eastern African MSA lithic assemblage composition, though they lacked the means to make similar developments in the characterisation of MSA environments, acknowledging the mismatched geographies and scales of archaeological and environmental records [18]. Blinkhorn and Grove [10,11] in a suite of quantitative analyses, brought together ecology and archaeology using an expanded dataset of MSA lithic artefact typology alongside modern environmental datasets and models for the Last Glacial Maximum (LGM) and Last Interglacial (MIS 5e). Their results stressed the influence of environmental settings over the spatiotemporal distribution of MSA sites, with pulsed patterns of occupation intensity occurring during interglacial stages [10]. Significant relationships between raw material and stone tool types and geographic and environmental variables were reported [11], with the strongest relationships with topographic ‘roughness’, emulating earlier hypotheses by King and Bailey [25]. These results validate the emphasis placed by earlier studies on ecology and the physical landscape [12]; however, it remains to be tested whether Blinkhorn and Grove’s [10,11] use of arid and humid models as representations of the extremes of variability observed within an interglacial-glacial cycle effectively characterise change throughout the MSA.

As such, our understanding of Middle to Late Pleistocene diachronic change has been greatly improved by high-resolution climatic records, whilst a series of regional syntheses of MSA assemblages has encouraged considerations of the ecological implications of prehistoric climate change [9], the quantitative assessment of MSA archaeology [13], and their integration [10,11]. However, lake cores offer very limited insights into spatial patterns of climate change due to the inability to extrapolate across the wider landscape, the difficulty of translating relative wet and dry proxies into tangible climatic or

ecological parameters, and the lack of directly associated, stratigraphically secure archaeological assemblages. Conversely, studies that rely on simplistic arid-humid simulated datasets [9–11] or use modern biogeographic zones to represent Pleistocene environments [13] lack chronological precision, and assume uniformity across successive glacial / interglacial cycles. Here we overcome such limitations to provide a sophisticated examination of the distribution and diversity of eastern African MSA assemblages through time and space within the context of Middle to Late Pleistocene climate change. We integrate novel high-resolution climate and biome simulations [26] with a database of chronometrically dated eastern African MSA stone tool assemblages [11] to refine the characterisation of MSA environments, map their extent across the landscape, and explore the role of environmental variability in structuring patterns of behaviour.

2. Results

2.1. Middle and Late Pleistocene climates of MSA assemblages

We first examined MSA assemblages (n = 84, Fig. 2) spanning the Middle to Late Pleistocene using simulated climate data (see Methods). We extracted mean annual temperature (bio01) and total annual precipitation (bio12) values from the climate model [26] within 50km radii around each assemblage, centred on its mid-age date range rounded to the nearest 1000 year (kyr) time slice, to characterise environments across the wider logistical landscape (following Blinkhorn and Grove [10,11]). The climatic conditions for each assemblage can be found in Supplementary Table S1 and are illustrated in Fig. 1.

We found that average temperatures at eastern African MSA assemblage varied between 9°C and 25°C, with most assemblages (n = 59) falling within the 68% confidence interval of 14–23°C. The warmest environments occupied were found in coastal regions, such as Abdur along the Red Sea coast of modern-day Eritrea (25°C) and Panga Ya Saidi situated on the Kenyan coast (24°C), as well as in the Lower Omo Valley of southwestern Ethiopia (24 – 23°C). These hot environments were inhabited during MIS 5 and MIS 7. On the other hand, the coldest environments inhabited were at high altitude, notably at Fincha Habera in the Bale Mountains of southern Ethiopia (9–10°C) and at the Kenyan Rift Valley assemblages of Marmonet Drift (10–14°C) and Enkapune ya Muto (13°C), with most of these occupations dating to MIS 3. Average precipitation levels experienced by Middle to Late Pleistocene MSA populations in eastern Africa ranged between 396mm and 1593mm, with most assemblages (n = 59) falling within the 68% confidence interval of 620-1150mm, corresponding to the precipitation bracket of sub-humid landscapes. The wettest habitats were located on islands within and along the shore of Lake Victoria at the sites of Rusinga Nyamtia (1593mm) and Karungu (1374-1499mm) in MIS 3 and 5, as well as within the Ethiopian Rift Valley at Gademotta (1368mm), the Ethiopian Highlands at Mochena Borango (1270-1297mm), and the Kenyan Rift Valley at Marmonet Drift (1173-1368mm) in MIS 3, 5 and 7. On the other hand, the driest occupations occurred at Laas Geel in Somaliland during MIS 3 (396mm) as well as within the Lower Omo Valley (534-582mm) during MIS 5 and 7.

2.2. Classifying biomes and ecotones

We then used the modelled biome dataset (biome4output) [26] to classify the local ecology of each MSA occupation with a 50km radius. We found that 38% of the assemblages (n = 32) had access to only tropical xerophytic shrubland within their logistical landscape, and a further 42% of assemblages with access to this biome within a 50km radius (n = 35). Figure 1 shows that tropical xerophytic shrubland was persistently occupied throughout the Middle to Late Pleistocene. The preferential occupation of tropical xerophytic shrubland (see Fig. 3. for modern examples) emphasises it as an important ecosystem for MSA populations. Eastern African MSA adaptive systems were likely specialised for engagement with tropical xerophytic shrubland, and its modulation may therefore have influenced patterns of Middle to Late Pleistocene human distribution. In total, 57% of the assemblages' logistical landscapes encompass the boundaries between multiple biomes (n = 48, see Supplementary Table S1 for details on ecotones for each assemblage). The majority of these ecotonal sites are situated between 'open' (i.e., tropical xerophytic shrubland, steppe tundra, desert, tropical savanna) and 'closed' (i.e., temperate conifer forest, tropical deciduous forest/woodland, warm mixed forest, temperate sclerophyll woodland) biome types, supporting the assertion of Basell [9] that access to wooded ecologies was important for MSA populations. The most common ecotone occupied during the eastern African MSA was that between tropical xerophytic shrubland and temperate conifer forest, which is seen as far north as Goda Butchia in southeastern Ethiopia, and as far south as Mumba in Tanzania. However, the region to the east of Lake Victoria shows the most intense occupation of this ecotone, the boundary of which fluctuates through time and space (see Supplementary Table S1 for percentages of biomes within 50km of each assemblage).

We found that MIS 7 saw the preferential occupation of closed ecotones between temperate conifer forest and warm mixed forest, as well as tropical xerophytic shrubland and associated ecotones which are generally occupied throughout the period. MIS 5 saw a slight increase in habitat diversity, though expansions primarily involved the tracking of tropical xerophytic shrubland environments (as shown by all assemblages in MIS 5 having access to this biome within 50km) with exposure to new ecotones occurring at the peripheries. This can be seen at assemblages distributed widely across the region; for example, certain occupations at Omo would have involved engagement with deserts alongside tropical xerophytic shrubland, whereas some MSA populations at Panga Ya Saidi had access to tropical deciduous forest and tropical savannah environments within their logistical landscape. MIS 3 saw the greatest variety in the biomes and ecotones occupied, where expansions can be seen into new and previously uninhabited environments, such as steppe tundra and warm mixed forest, with a distinct emphasis on temperate conifer forest rather than tropical xerophytic shrubland.

2.3. Characterising environments during the Middle to Late Pleistocene

We used cluster analyses to group the assemblages based on their climatic values to assess patterns in habitat choice. To do this, we scaled and combined the temperature and precipitation data and employed

an automated clustering algorithm (the average silhouette method) to ascertain the optimal number (k) of clusters in the data. The algorithm found ten clusters to represent the best division of the data (see Fig. 4, Supplementary Fig. S1).

Most of the assemblages (n = 45) fall within warm to temperate sub-humid clusters (2,4,5 and 7) with a broad temperature range of 13–19°C and a precipitation range of 613-1297mm. These clusters are dominated by tropical xerophytic shrubland and temperate conifer forest environments and their ecotones. We found that overall only 2 clusters (8,9) did not include assemblages with access to tropical xerophytic shrubland, indicating that this biome was present across a large portion of the MSA climatic range, except at the coldest extreme. We found that the coldest cluster, cluster 9 (temperature range 9–10°C), was the most ecotonal, with all assemblages situated at high altitude where populations would have had access to steppe tundra, temperate conifer forest, temperate sclerophyll woodland and warm mixed forest, the complex topography allowing diverse biomes to appear closer together than is usually possible [27]. Extremely humid assemblages from around Lake Victoria (Karungu and Rusinga Nyamita) formed cluster 10 (1374-1593mm precipitation). These assemblages have moderate temperatures (16–18°C) and occupy an ecotone between tropical xerophytic shrubland and temperate conifer forest. Panga Ya Saidi and Laas Geel form their own respective clusters (3 and 6) due to their distinctively hot temperatures; however, at Panga Ya Saidi, this is coupled with moist sub-humid conditions and a diverse tropical environment (24°C, 996-1153mm), whereas Laas Geel possesses the lowest annual precipitation of all the assemblages (18°C, 396mm), making its hot-dry environment unique for the eastern African MSA. However, the assemblage at Laas Geel falls within the tropical xerophytic shrubland biome, with access to some open conifer woodland within 50km, suggesting that whilst occupying a climatic extreme, this distinct habitat represents an extension of the types of environments that eastern African MSA populations were already well adapted to.

2.4. Phased habitability models

We used the precipitation and temperature data from the assemblages as the parameters to produce phased ‘habitability’ models for abundantly populated interglacial phases of the MSA, demonstrating the extent of the landscape that experienced comparable settings to assemblages dated within that period. The climatic range produced by each phased subset was projected throughout every 1000-year time interval for that MIS, and then the percentage of ‘habitable’ cells (i.e., cells that remain within that climatic range) was calculated to identify areas that were persistently habitable, as well as the geographic range and temporal scope of impersistent habitable landscapes.

Figure 5 demonstrates the temperature, precipitation, and combined habitability models for each phase. MIS 9 shows the most limited habitable zone out of the interglacial phases, partially due to the lower number of assemblages available to construct the models. MIS 7 marks a period of expansion, with the region surrounding Lake Victoria and the Eastern Rift Valley Lakes and the Ethiopian Highlands showing the most persistent habitability across the region. For temperature, large areas of the Horn and modern-day Sudan show less persistent habitability (*ca.* 40–50% of MIS 7), with pockets of unsuitability along the coast of the Baab el Mandeb and the border between modern-day Ethiopian and Somalia. However,

arid zones of the southern Sahara are completely uninhabitable in terms of precipitation (0% habitable), as is the tip of the Horn. Precipitation is thus the limiting factor when considering habitability for MIS 7. MIS 5 sees the largest increase in habitable area for temperature, with all cells showing comparable temperature values for at least 60% of the period. Precipitation habitability is however more fragmented, with pockets of uninhabitability forming around the northeast edge of Lake Victoria, in the region to the south of Lake Tana, and within modern-day Tanzania. Like MIS 7, this means that habitability is limited by precipitation in MIS 5 albeit towards the more humid extreme. However, the habitability models for MIS 3 demonstrates the opposite pattern. Temperature habitability show the most restricted distribution of all the models, with habitable areas concentrated to the areas around Lake Victoria and the Ethiopian highlands, which are linked towards the southeast of Lake Turkana. Yet, MIS 3 shows the most persistent and widely distributed zone of habitability for precipitation, where much of eastern Africa, except towards the Sahara and the very tip of the Horn of Africa, remains persistently within the range of precipitation values experienced by MIS3 occupations. Overall, these models propose that interglacial MSA occupations, especially in MIS 5, may have been much more spatially diverse than presently known.

2.5. Exploring the relationship between climate and Middle Stone Age assemblages

We then examined the extent to which patterns of variability in stone tool assemblage composition and raw material use correlated with environmental conditions within a 50km radius at the mid-age of occupation of each assemblage, as well as a suite of other variables recorded by Blinkhorn and Grove [11] (see Methods and Supplementary Methods S1 details). Figure 6 demonstrates the relationships between these variables and toolkit composition and raw material use, revealed using simple Mantel tests (Table 1 and Supplementary Table S3-4). We found that MSA assemblage composition was correlated with differences in both mean annual temperature (adj. p = 0.001; Table 1) and total annual precipitation (adj. p = 0.003; Table 1), and raw material use also shows statistically significant relationships with both mean annual temperature (adj. p = 0.001; Table 1) and total annual precipitation (adj. p = 0.003; Table 1). With the use of Pleistocene climate models at high temporal resolutions, these results refine the findings of Blinkhorn and Grove [11], which relied on comparisons of the climatic extremes of the LGM and LIG.

Table 1
Simple Mantel test results for the effects of precipitation and temperature on toolkit composition and raw material. Statistical significance highlighted at $p < 0.05$ (*) or $p < 0.01$ (**). The Benjamini-Hochberg procedure was used to adjust p values.

	Toolkit composition			**Raw material**		
	Coefficient	p	Adj. p	Coefficient	p	Adj. p
Precipitation	0.1972	0.001**	0.003**	0.1587	0.001**	0.003**
Temperature	0.2144	0.001**	0.003**	0.1532	0.001**	0.001**

We next employed multiple matrix regressions to resolve independent, significant correlations between differences in either stone tool assemblage composition or raw material use, and differences across the different variables. Table 2 demonstrates that four variables exhibit independent significant effects on toolkit composition ($F = 68.0$, multiple $R^2 = 0.15$, $p = 0.001$) - raw material choice, roughness, site type and precipitation. In the multiple matrix regression for raw material (Table 2), five variables were found to have independent effects ($F = 54.8$, multiple $r^2 = 0.12$, $p = 0.001$) – toolkit composition, cost path, roughness and simple age, with precipitation being very close to significant. In each instance, these results complement earlier findings, but the use of highly resolved climate models illustrates the independent and significant relationship between MSA behaviour and precipitation that was not evident from previous analyses that were reliant on models for climatic extremes [11]. This highlights the benefit of using highly chronologically resolved model data to more accurately characterise the climatic parameters of MSA occupations in eastern Africa and to reveal the relationship between environmental and behavioural variability.

Table 2
Multiple matrix regression results for toolkit composition and raw material. Descriptions of each variable can be found in the Supplementary Methods. Statistical significance highlighted at $p < 0.05$ (*) or $p < 0.01$ (**).

	Toolkit composition		Raw material	
	Coefficient	p	Coefficient	p
Toolkit composition	NA	NA	0.3119	0.001**
Raw material	0.1483	0.001**	NA	NA
Method	0.009	0.698	0.0351	0.192
Site type	0.0328	0.018*	-0.0061	0.7
Simple Age	0.0184	0.668	0.149	0.007**
Cost path	0.0172	0.669	0.1991	0.001**
Altitude	-0.09	0.473	0.2206	0.106
Roughness	0.2645	0.004**	-0.2286	0.017*
Temperature	0.0673	0.298	-0.0108	0.896
Precipitation	0.111	0.015*	0.1124	0.053

3. Discussion

Using high-resolution modelled climatic data, we have conducted more sophisticated analyses of the environments inhabited by MSA-making populations than was previously possible, bridging former disconnects between archaeological and climatic records within a spatiotemporally explicit framework.

Figure 1 highlights the challenge of generalising from proxy core records which we have overcome through the parameterisation of temperature and precipitation with simulated models, revealing interpretable patterns in terms of MSA assemblage environments. Our analyses have extended previous work applying models of the LGM and LIG to represent climatic extremes [10,11] and importantly have revealed the climatic bracket of eastern African MSA occupations to around 9–25°C mean annual temperature and 396-1593mm total annual precipitation. MSA assemblages are more prevalent during interglacial phases (MIS 3, 5, and 7) and we found that populations during these periods inhabited more diverse and widely distributed environments. Most assemblages are located within or with access to tropical xerophytic shrubland, and usually are found within proximity to at least one forest or woodland biome. Using spatiotemporally explicit models we also established that precipitation levels experienced by MSA populations had an impact on both behavioural variability and the use of raw materials, which we explore further here using penalised logistic regression.

Our results highlight spatial and diachronic trends in the environments inhabited by eastern African MSA populations, which are demonstrated by Fig. 1, 3 and Supplementary Table S1. MIS 9 and 8 saw occupations that were typical for the eastern African MSA in terms of temperature, precipitation, altitude, and biomes inhabited. During MIS 7, there was a dramatic increase in the environments occupied, spanning much of the climatic range of the later interglacial phases with emphasis on forest/woodland ecotones and tropical xerophytic shrubland. MIS 6 saw the occupation of a cold, high-altitude environment; however, the phase is only represented by a single assemblage, Marmonet Drift_H2, with a large date range so we do not place too much emphasis on its mid-age climatic placement. MIS 5 was marked by another phase of expansion, though with limited presence in woodland habitats and typically warmer, drier and low altitude occupations. MIS 5 has been proposed to represent a transitional point within the MSA stone tool record, due to the augmentation of MSA toolkits with new combinations of stone tools and the colonisation of different landscapes into the Late Pleistocene [9,10,13]. Engagement with these new environments likely occurred at the edge of the logistical landscape, with many eastern African MSA assemblages falling on ecotonal boundaries between tropical xerophytic shrubland and previously unoccupied biome types. An example of this is found with the youngest MSA occupation at Panga Ya Saidi, which is placed at a unique tropical ecotone [28]. MSA occupation of Panga Ya Saidi at the end of MIS 5 is rapidly followed by cultural change, with the appearance of the Later Stone Age here occurring earlier than anywhere else in the region [29]. New constellations of tools within MIS 5 toolkits suggest corresponding changes in behaviour previously unseen in the MSA [10], which perhaps may have been key for these expansions beyond tropical xerophytic shrubland. Together, this suggests that certain MSA toolkits may have led to adaptation, as opposed to adaptations being a pre-requisite for expansion, with transient ecotonal habitats requiring the adoption of a range of survival strategies and potentially mediating interaction between different groups across different environmental contexts [2,28,29]. Assemblages dated to MIS 4 show a climatic range close to that of MIS 3, where we see a push into higher precipitation woodland habitats with a limited change in temperature and altitude. Habitability modelling for MIS 3 suggests that temperature, rather than precipitation as seen during earlier interglacial periods, constrained expansions into new landscapes. Assemblages across the Middle to Late

Pleistocene exhibited comparable levels of temperature variability (MIS 3 = 9–19°C, MIS 5 = 13–25°C, MIS 7 = 12–23°C), however MIS 3 saw a notable extension of the habitable precipitation regime and the occupation of both more arid and humid environments, though this was limited to within the MSA temperature range.

Eastern African MSA assemblages are primarily located within tropical xerophytic shrubland, characterised by arid-adapted species such as that from the *Acacia and Commiphora* genera. Whilst it is the most abundant biome across modern eastern Africa, and likely also so during the Pleistocene, the intense occupation of tropical xerophytic shrubland and its associated ecotones suggests that eastern African MSA adaptive strategies were centred around engaging with subsistence resources associated with this biome. Our results also confirm the importance of wooded ecotones for sustaining MSA populations [9], with the most common ecotone occurring between temperate conifer forest and tropical xerophytic shrubland, distributed widely across the region though most concentrated towards the eastern edge of Lake Victoria and the associated region, where most assemblages occupy ecotones between tropical xerophytic shrubland and various forested/woodland biomes. Today, Lake Victoria sits on the junction between central African rainforests and savanna habitats to the east, forming an important boundary for large mammal [30] and human [31] populations. Our phased models (Fig. 5) propose that the region to the east of Lake Victoria would have seen sustained and persistent occupation throughout the Middle to Late Pleistocene in the face of climatic fluctuation, implicating it as a potential refugium for hominins in eastern Africa. The availability of freshwater provided by surrounding rivers and springs [32] and the complex topography of the Rift Valley [25, 33] may also have helped buffer against the strongest effects of climate change in the area [18]. Occupying refugia likely required minimal cultural adaptation to environmental change, which could explain why assemblages from within the Lake Victoria basin show distinct differences from the general eastern African MSA [34]. Moreover, Lake Victoria, which is a relatively young lake but estimated to exist by 500 – 400 kya [35], is the source of the White Nile, and therefore its refugial position could also have interesting implications for dispersals from the region out of the continent [36]. Together, this highlights the potential role of refugia in structuring MSA human cultural and biological diversity [3,4], laying the critical foundations for later human evolution.

Beyond simply characterising MSA assemblage environments and ecologies, our use of matrix correlations presents an important means to examine the extent to which climatic features influenced behaviour, here characterised by stone tool assemblage composition. Our results firstly demonstrate that precipitation has a significant, independent effect on toolkit composition; further examination via binary logistic regression shows statistically significant decreases in the probability of backed microliths, borers, centripetal technology, platform cores, and scrapers occurring in assemblages as precipitation levels increase, after controlling for all other variables in the analysis (see Supplementary Methods S2 and Supplementary Table S2). Some of these tool types have been found to be significant indicators of either Later Stone Age (backed pieces) or MSA (scrapers) toolkits [37], [38], perhaps linking an increase in precipitation tolerance to the development of the LSA, as documented at Panga Ya Saidi. Roughness also has a significant impact on toolkit compsition, with further analyses demonstrating that the probability of backed microliths and Levallois blades, points, and flakes occurring in assemblages decreases as the

energetic demands of the environment increase. Further analysis of the site type variable demonstrates that it has significant effects on the probability of backed microliths, bipolar technology, and Levallois flakes appearing in assemblages, with all these technologies occurring more frequently in cave or rock shelter sites. Finally, there are numerous independent effects of the use of particular raw materials on the presence of individual technologies in the assemblages, as summarised in Supplementary Table S2. We also found precipitation has an independent effect on raw material use, alongside cost path, roughness, simple age and toolkit composition. This constellation of geographic-based variables suggests a complex pattern of spatial autocorrelation, likely grounded in the local availability of raw materials across the landscape. Overall, these results demonstrate a complex interaction between the environment and MSA behaviour, with the energetic requirements of the physical landscape and local precipitation regimes likely requiring different constellations of tools from the MSA toolkit.

4. Conclusion

The MSA record of eastern Africa is fundamental for the exploration of ideas surrounding the role of climate change and the environment in recent human evolution and dispersals within and beyond the continent. Our application of high-resolution paleoenvironmental reconstructions has enabled a previously impossible characterisation of the ecosystems inhabited by early human populations, highlighting a wide range of inhabited environments far beyond those assumed by classic habitat-specific hypotheses for human evolution [39–42]. By establishing the role of shifting environmental conditions and ecological boundaries on the distribution and variability of dated MSA assemblages, our work also helps illuminate some of the processes that shaped behavioural diversity during this key period, such as that MSA toolkits likely facilitated expansions into diverse environments, adding further complexity to within-region migration than environment tracking [43]. Understanding this complex interaction between population dynamics, dispersals, cultural evolution and the environment is also key to moving beyond simplistic single-origin models in favour of more complex reticulate models for recent human evolution [3,4].

5. Materials And Methods

We employed here simulated climate and biome reconstructions for the past 800 ka [26]. Mean annual temperature (bio01), total annual precipitation (bio12) and biome (biomeoutput04) were extracted from the model for 1000 year time slices and stored in a raster stack using the ‘raster’ R package [44]. We then selected the time slices corresponding to the mid-age of each assemblage, rounded to the nearest 1000 years to match the resolution of the climate data. Each time slice was cropped according to the predicted sea level for that period, using global sea-level change data [45] (see Supplementary Methods S3).

We integrated the climate model with an archaeological dataset reported in Blinkhorn and Grove [11] which comprises presence/absence data of 16 tool types and 8 raw material types for eastern African MSA assemblages, as well as other typological characteristics, such as site type and method of excavation (see Supplementary Methods S1 for further description).

5.1. Refining the climatic parameters

We extracted temperature and precipitation values [26] in 50km radius buffers around the coordinates of each assemblage from its mid-age time slice, representing the home range sizes of hunter-gatherer populations [46] and regional patterns of raw material procurement [47, 48]. In order to better characterise patterns of landscape variability across this range, we downscaled model datasets from 30' to 2.5' by resampling the data using bilinear interpolation, following examination of alternate methods (see Supplementary Methods S4). We calculated the mean and standard deviation of the values across the 50km buffer for each assemblage.

5.2. Cluster analyses

Dissimilarity matrices for the temperature and precipitation data were calculated using the Euclidean distance. Hierarchical clustering of the dissimilarity matrices was then employed to examine grouping of assemblages according to temperature and precipitation combined in equal combinations to characterise environments, following Blinkhorn and Grove [10]. Cluster analysis iteratively merges cases into a group using a measure of closeness (i.e., the opposite of dissimilarity). We applied the average silhouette method, which uses k-means clustering to automatically determine the optimal number of clusters from the data. The average silhouette method evaluates the quality of clustering by determining how well each assemblage lies within its cluster, producing a measure of how similar an assemblage is to its own cluster relative to other clusters. We created a dendrogram of the assemblages (Fig. 4) which was cut according to the k-means output (k = 10) to define our clusters.

5.3. Biome classification

To classify the biomes occupied by each assemblage, we used the modelled biome dataset [26]. To increase the resolution of the data to 2.5', we resampled the raster layers using the nearest neighbour method, which is most suitable for categorical data. We extracted the biome type for each assemblage location at its mid-age and then recorded the number of cells (each representative of 4.63km) assigned to each biome within a 50km radius around each assemblage.

5.4. Phased climate suitability models

We used the temperature and precipitation values from within a 50km of each assemblage to produce phased models of 'habitability'. To do this, we subsetted the assemblages according to MIS, and produced a series of climatic ranges based on the inhabited temperature and precipitation values during that period. We then calculated the percentage of time slices within each MIS that fall within the climatic range of assemblages dated to that period. This produced phased models mapping the areas of the landscape that would have been comparable to those inhabited during that MIS, indicating the degree of habitat stability over time.

5.5. *Mantel tests and multiple matrix regression*

To explore the relationships between toolkit diversity, raw material choice and environments, we used simple Mantel tests and multiple matrix regression, the null hypothesis for which assumes that there is no correlation between two distance matrices (e.g., toolkit composition and temperature), factoring in the impact of additional variables (e.g., raw material) for multiple matrix regressions. Positive correlation in dissimilarity between two distance matrices, like toolkit composition and temperature, would suggest that assemblages experiencing similar temperatures share more similar constellations of tool types, whereas a negative correlation would suggest that as dissimilarity increases in one variable, it decreases in another.

As described in Blinkhorn and Grove [11], the additional distance matrices used as variables that may explain variation in MSA toolkits for multiple matrix regression are site type, method, simple age (mid-age), cost path (a measure of physical distance). altitude within 50km and roughness within 50km (calculated as amount of energy needed to move across the logistical landscape). A description of how each distance measure was calculated can be found in the Supplementary Methods S4, following Blinkhorn and Grove [11]. Simple Mantel tests were conducted using the 'vegan' R package [49], employing 999 permutations to obtain p-values. The Benjamini-Hochberg procedure was used to adjust p values. Multiple matrix regression was performed with 999 permutations using the 'phytools' package in R [49]. Additional binary logistic regressions using penalized maximum likelihood were conducted to determine the effects of significant predictors on individual technologies using the 'brglm' R package [51].

Declarations

Data availability

The datasets used in this study are all freely available [11], [26], [44], [52]. R code for the analyses presented will be published at https://osf.io/nxfer/ upon acceptance and are presented as Supplementary Material for the purposes of the review process.

Acknowledgements

LT is supported by an Arts and Humanities Research Council studentship (AH/R012792/1). AM is supported by a Consolidator ERC grant (647797): "LocalAdaptation". We would like to thank John Gowlett for his comments on this manuscript.

Author contributions

LT, MG and JB conceptualised and designed the project. LT, MG, JB and AM acquired the data. LT, MG and JB performed the analysis. LT, MG, JB and SR produced the figures. All authors interpreted the results, and wrote and reviewed the manuscript.

Competing interests

The author(s) declare no competing interests.

References

1. Shea, J. J. *Prehistoric Stone Tools of Eastern Africa: A Guide*. Cambridge: Cambridge University Press, (2020).
2. Hijmans, R. J. *et al.* 'raster': Geographic Data Analysis and Modeling. CRAN: R Packages: https://cran.r-project.org/web/packages/raster/index.html. (2021).
3. Spratt, R. M. & Lisiecki, L. E. A Late Pleistocene sea level stack. *Clim. Past*, **12**, 1079–1092 https://doi.org/10.5194/cp-12-1079-2016 (2016).
4. Binford, L. R. *Constructing frames of reference: an analytical method for archaeological theory building using ethnographic and environmental datasets* (University of California Press, Berkeley, 2001).
5. Blegen, N. The earliest long-distance obsidian transport: Evidence from the ~200 ka Middle Stone Age Sibilo School Road Site, Baringo, Kenya. *J. Hum. Evol*, **103**, 1–19 https://doi.org/10.1016/j.jhevol.2016.11.002 (2017).
6. Faith, J. T. *et al.* Paleoenvironmental context of the Middle Stone Age record from Karungu, Lake Victoria Basin, Kenya, and its implications for human and faunal dispersals in East Africa. *J. Hum. Evol*, **83**, 28–45 https://doi.org/10.1016/j.jhevol.2015.03.004 (2015).
7. Oksanen, J. *et al.* 'vegan': Community Ecology Package. CRAN: R Packages: https://cran.r-project.org/web/packages/vegan/index.html (2020).
8. Revell, L. J. phytools: an R package for phylogenetic comparative biology (and other things). *Methods Ecol. Evol*, **3** (2), 217–223 https://doi.org/10.1111/j.2041-210X.2011.00169.x (2012).
9. Kosmidis, I. & 'brglm' Bias reduction in binary-response Generalized Linear Models. CRAN: R Packages: https://cran.r-project.org/web/packages/brglm2/brglm2.pdf (2007).
10. The General Bathymetric Chart of the Oceans (GEBCO). Gridded Bathymetry Data. Available online at: https://www.gebco.net/data_and_products/gridded_bathymetry_data/ (2020).
11. Lisiecki, L. E. & Raymo, M. E. A Pliocene-Pleistocene stack of 57 globally distributed benthic δ18O records., **20**, 1–17 https://doi.org/10.1029/2004PA001071 (2005).
12. Trauth, M. H. *et al.* Recurring types of variability and transitions in the ~620 kyr record of climate change from the Chew Bahir basin, southern Ethiopia. *Quat. Sci. Rev*, **266**, 106777 https://doi.org/10.1016/j.quascirev.2020.106777 (2021).
13. Muiruri, V. M. *et al.* A million year vegetation history and palaeoenvironmental record from the Lake Magadi Basin, Kenya Rift Valley. *Palaeogeogr. Palaeoclimatol. Palaeoecol*, **567**, 110247 https://doi.org/10.1016/j.palaeo.2021.110247 (2021).

14. Lyons, R. P. *et al.* Continuous 1.3-million-year record of East African hydroclimate, and implications for patterns of evolution and biodiversity. Proc. Nat. Acad. Sci. USA. 112(51), 15568–15573(2015). https://doi.org/10.1073/pnas.1512864112
15. Jouzel, J. *et al.* Orbital and Millennial Antarctic Climate Variability over the Past 800,000 Years. *Science, ***317**(5839),793–796, (2007). 10.1126/science.1141038
16. Laskar, J. *et al.* A long-term numerical solution for the insolation quantities of the Earth. *Astron. Astrophys*, **428**, 261–285 https://doi.org/10.1051/0004-6361:20041335 (2004).
17. Trauth, M. H. *et al.* Human evolution in a variable environment: The amplifier lakes of Eastern Africa. *Quat. Sci. Rev.* **29** (23–24), 2981–2988, (2010). 10.1016/j.quascirev.2010.07.007
18. Blome, M. W., Cohen, A.S., Tryon, C. A., Brooks, A. S. & Russell, J. The environmental context for the origins of modern human diversity: A synthesis of regional variability in African climate 150,000–30,000 years ago. *J. Hum. Evol.***62**(5), 563–592, (2012). 10.1016/j.jhevol.2012.01.011
19. Lamb, H. F. *et al.*, 150,000-year palaeoclimate record from northern Ethiopia supports early, multiple dispersals of modern humans from Africa. *Sci. Reports* **8**, 1077, (2018). 10.1038/s41598-018-19601-w
20. Potts, R. *et al.* Increased ecological resource variability during a critical transition in hominin evolution. *Nature***6**(43), (2020). 10.1126/sciadv.abc8975
21. Lupien, R. L. *et al.* Eastern African environmental variation and its role in the evolution and cultural change of Homo over the last 1 million years. *J. Hum. Evol.* **157**, 103028, (2021). 10.1016/j.jhevol.2021.103028
22. Owen, R. B. *et al.* Progressive aridification in East Africa over the last half million years and implications for human evolution. *Proc. Natl. Acad. Sci.* **115(**44), 11174–11179, (2018). 10.1073/pnas.1801357115
23. Schaebitz, F. *et al.* Hydroclimate changes in eastern Africa over the past 200,000 years may have influenced early human dispersal. *Commun. Earth Environ.* **2**, 123**,** (2021). 10.1038/s43247-021-00195-7
24. Vidal, C. *et al.* Age of the oldest *Homo sapiens* from eastern Africa. Preprint at: 10.21203/rs.3.rs-373661/v1(2021).
25. King, G. & Bailey, G. N. Tectonics and human evolution. *Antiquity*, **80**(308), 265–286, (2006). 10.1017/S0003598X00093613
26. Krapp, M., Beyer, R. M., Edumundson, S. L., Valdes, P. J. & Manica, A. A statistics-based reconstruction of high-resolution global terrestrial climate for the last 800,000 years. *Sci. Data* 8, *228*, (2021). 10.1038/s41597-021-01009-3
27. Foley, R. A. *Humans Before Humanity.* Blackwell Publishing Inc. (1995).
28. d'Errico, F. *et al.* Trajectories of cultural innovation from the Middle to Later Stone Age in Eastern Africa: Personal ornaments, bone artifacts, and ocher from Panga ya Saidi, Kenya. *J. Hum. Evol*, 141, 102737, (2020). 10.1016/j.jhevol.2019.102737

29. Shipton, C. *et al.* 78,000-year-old record of Middle and Later stone age innovation in an East African tropical forest. *Nat. Commun.* 9, 1832, (2018). 10.1038/s41467-018-04057-3
30. Tryon, C. A. *et al.*, The Pleistocene prehistory of the Lake Victoria basin. *Quat. Int.* **404** (Part B), 100–114, (2016). 10.1016/j.quaint.2015.11.073
31. Lewis, M. *Ethnologue: Languages of the World*. Sixteenth. Texas: SIL International, (2009).
32. Cuthbert, M. O. *et al.* Modelling the role of groundwater hydro-refugia in East African hominin evolution and dispersal. *Nat. Commun.* **8**, 15696, (2017). 10.1038/ncomms15696
33. Ambrose, S. H. Middle and Later Stone Age Settlement Patterns In The Central Rift Valley, Kenya: Comparisons And Contrasts. In: *Settlement Dynamics of the Middle Palaeolithic and Middle Stone Age* (ed. N. J. Conard), pp. 21–43, (2001).
34. Tryon, C. A. The Middle/Later Stone Age transition and cultural dynamics of late Pleistocene East Africa. *Evo. Anthropol.* 28(5), 267–282, (2019). 10.1002/evan.21802
35. Williams, M. The Nile Basin: Quaternary geology, geomorphology and prehistoric environments. Cambridge: Cambridge University Press. (2019).
36. Beyer, R. M., Krapp, M., Eriksson, A. & Manica, A. Climatic windows for human migration out of Africa in the past 300,000 years. *Nat. Commun.* **12***,* 4889, (2021). 10.1038/s41467-021-24779-1
37. Grove, M. & Blinkhorn, J. Neural networks differentiate between Middle and Later Stone Age lithic assemblages in eastern Africa. *PLoS One* **15**(8), e0237528, (2020). 10.1371/journal.pone.0237528
38. Grove, M. & Blinkhorn, J. Testing the Integrity of the Middle and Later Stone Age Cultural Taxonomic Division in Eastern Africa. *J. Paleolit. Archaeol.* **4**, 14, (2021). 10.1007/s41982-021-00087-4
39. Dart, R. A. *Australopithecus africanus*: the man-ape of South Africa. *Nature* 115, 195–199, (1925). 10.1038/115195a0
40. Dart, R. A. The predatory transition from ape to man. *Int. Anthr. Ling. Rev 1*, 201–218, (1953).
41. Washburn, S. L. Tools and human evolution. *Sci. Am.* **203**, 63–75, (1960). 10.1038/scientificamerican0960-62
42. Rayner, R. J., Moon, B. P. & Masters, J. C. The Makapansgat australopithecine environment. *J. Hum. Evol.* **24**(3), 219–231, (1993). 10.1006/jhev.1993.1016
43. Mirazón Lahr, M. & Foley, R. A. Towards a Theory of Modern Human Origins: Geography, Demography, and Diversity in Recent Human Evolution. *Am. J. Phys. Anthropol.* **107**(S27), 137–76, (1998). 10.1002/(SICI)1096–8644(1998)107:27 + < 137::AID-AJPA6 > 3.0.CO;2-Q
44. Hijmans, R. J. *et al*. 'raster': Geographic Data Analysis and Modeling. CRAN: R Packages: https://cran.r-project.org/web/packages/raster/index.html. (2021).
45. Spratt, R. M. & Lisiecki, L. E. A Late Pleistocene sea level stack. *Clim. Past*, **12**, 1079–1092, (2016). 10.5194/cp-12-1079-2016
46. Binford, L. R. *Constructing frames of reference: an analytical method for archaeological theory building using ethnographic and environmental datasets*. Berkeley: University of California Press, (2001).

47. Blegen, N. The earliest long-distance obsidian transport: Evidence from the ~200 ka Middle Stone Age Sibilo School Road Site, Baringo, Kenya. *J. Hum. Evol.* **103**, 1–19, (2017). 10.1016/j.jhevol.2016.11.002
48. Faith, J. T. *et al.* Paleoenvironmental context of the Middle Stone Age record from Karungu, Lake Victoria Basin, Kenya, and its implications for human and faunal dispersals in East Africa. *J. Hum. Evol.* **83**, 28–45, (2015). 10.1016/j.jhevol.2015.03.004
49. Oksanen, J. *et al.* 'vegan': Community Ecology Package. CRAN: R Packages: https://cran.r-project.org/web/packages/vegan/index.html (2020).
50. Revell, L. J. phytools: an R package for phylogenetic comparative biology (and other things). *Methods Ecol. Evol.* **3**(2), 217–223, (2012). 10.1111/j.2041-210X.2011.00169.x
51. Kosmidis, I. 'brglm': Bias reduction in binary-response Generalized Linear Models. CRAN: R Packages: https://cran.r-project.org/web/packages/brglm2/brglm2.pdf (2007).
52. The General Bathymetric Chart of the Oceans (GEBCO). Gridded Bathymetry Data. Available online at: https://www.gebco.net/data_and_products/gridded_bathymetry_data/ (2020).
53. Lisiecki, L. E. & Raymo, M. E. A Pliocene-Pleistocene stack of 57 globally distributed benthic δ18O records. *Paleoceanography* **20**, 1–17, (2005). 10.1029/2004PA001071
54. Trauth, M. H. *et al.* Recurring types of variability and transitions in the ~620 kyr record of climate change from the Chew Bahir basin, southern Ethiopia. *Quat. Sci. Rev.* **266**, 106777, (2021). 10.1016/j.quascirev.2020.106777
55. Muiruri, V. M. *et al.* A million year vegetation history and palaeoenvironmental record from the Lake Magadi Basin, Kenya Rift Valley. *Palaeogeogr. Palaeoclimatol. Palaeoecol.* **567**, 110247, (2021). 10.1016/j.palaeo.2021.110247
56. Lyons, R. P. *et al.* Continuous 1.3-million-year record of East African hydroclimate, and implications for patterns of evolution and biodiversity. *Proc. Nat. Acad. Sci. USA*. 112(51), 15568–15573, (2015). https://doi.org/10.1073/pnas.1512864112
57. Jouzel, J. *et al.* Orbital and Millennial Antarctic Climate Variability over the Past 800,000 Years. *Science, *__317__(5839), 793–796, (2007). 10.1126/science.1141038
58. Laskar, J., Robutel, P., Joutel, F., Gastineau, M., Correia, A. C. M. & Levrard, B. A long-term numerical solution for the insolation quantities of the Earth. *Astron. Astrophys.* **428**, 261–285, (2004). 10.1051/0004-6361:20041335

Figures

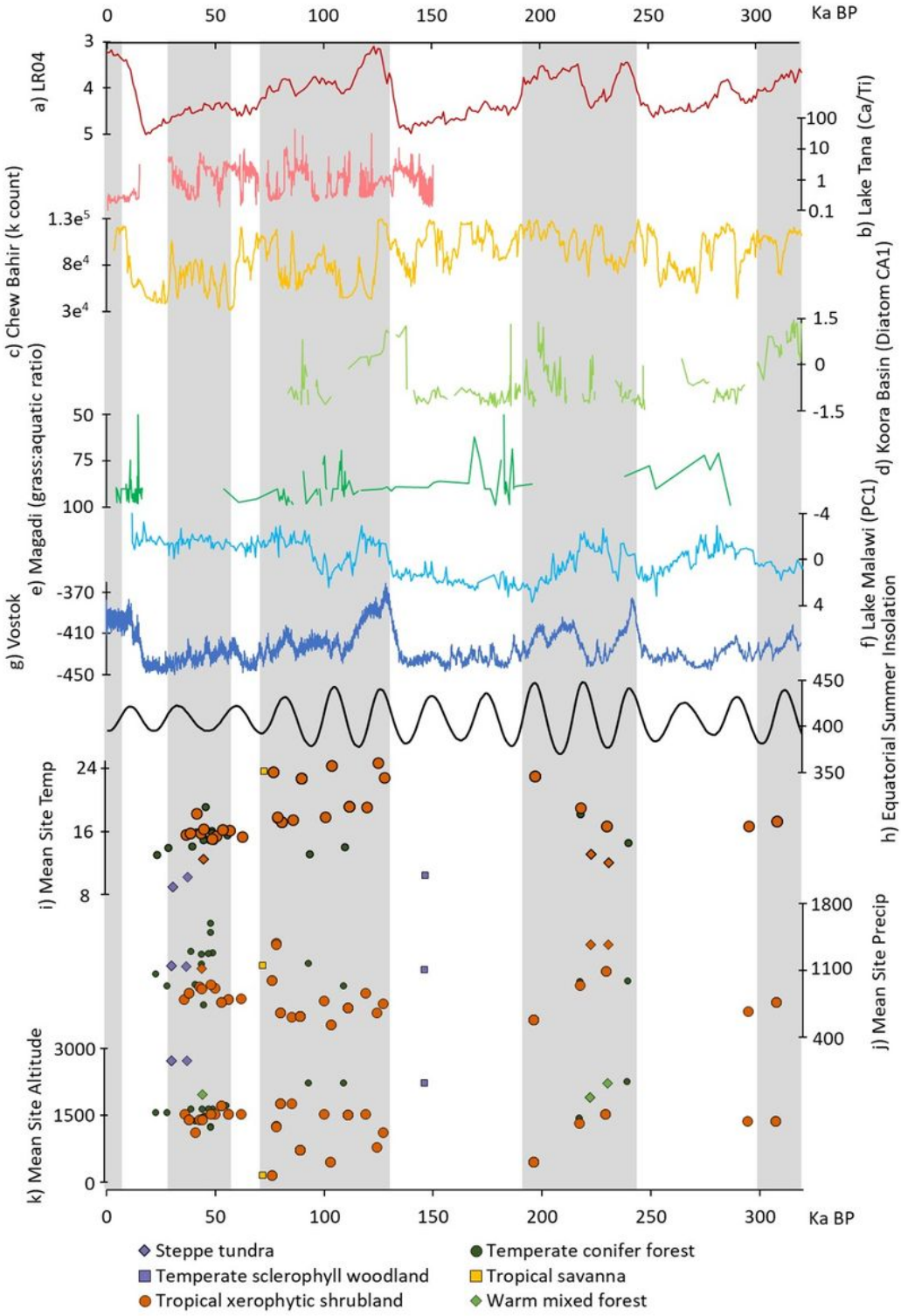

Figure 1

Composite of key inter-regional and regional climatic records, insolation, and temperature, precipitation and altitude parameters for dated eastern African Middle Stone Age assemblages including (a) LR04 Benthic Stack δ18O [53]; (b) Lake Tana Ca/Ti ratio [19]; (c) Chew Bahir k-counts [54]; (d) Koora Basin diatom CA [20]; (e) Magadi Pollen grass:aquatic ratio [55]; (f) Lake Malawi PC1 [56]; (g) Vostok δD [‰ SMOW] [57]; (h) mean Equatorial summer (Jun-Aug) insolation (W/m2) [58]; mean (i) temperature (°C), (j)

precipitation (mm), and (k) altitude (meters above sea level) within 50km radius of eastern African MSA assemblages, illustrated at the mid-age point for each assemblage and symbolised according to its biome classification. Grey vertical bars indicate odd-numbered Marine Isotope Stages.

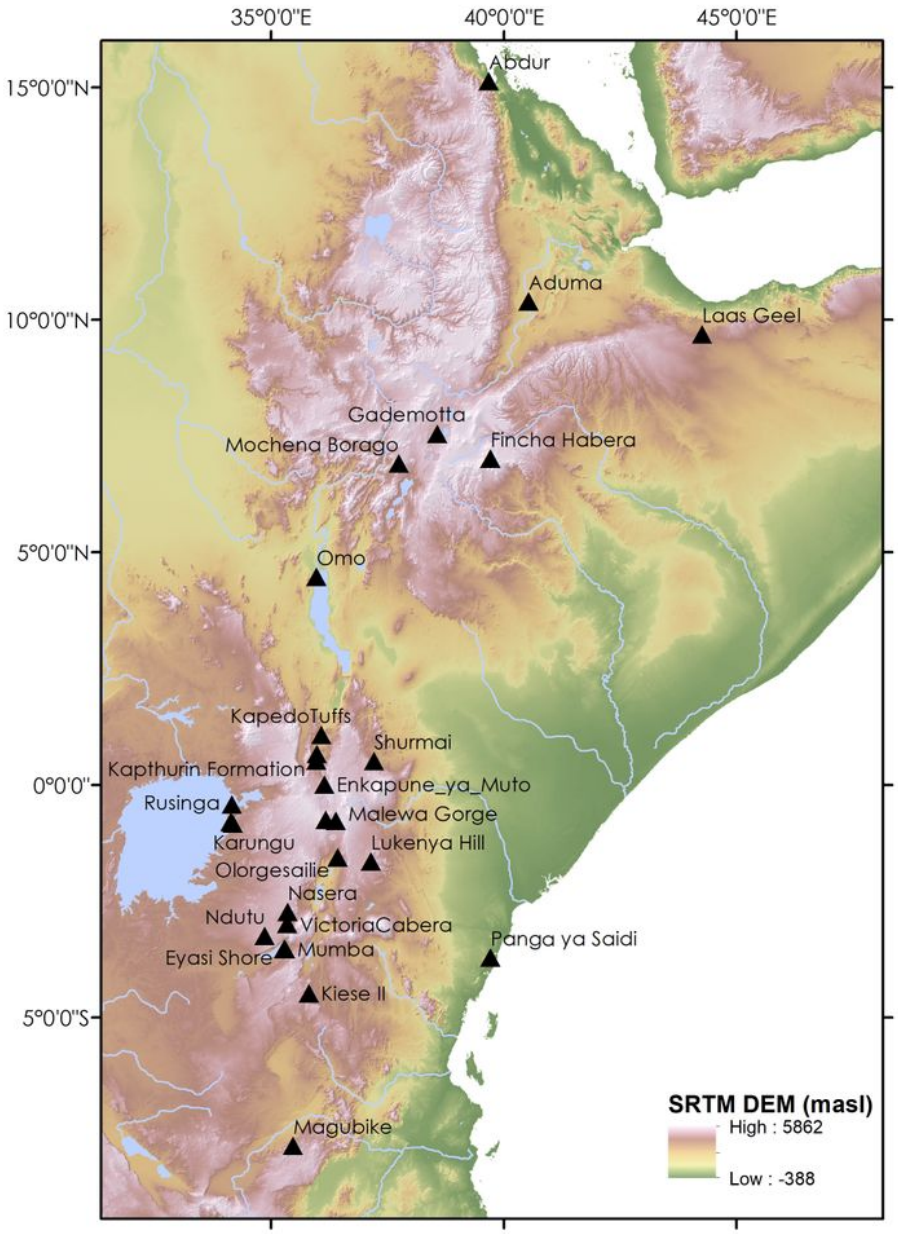

Figure 2

Distribution of the eastern African Middle Stone Age assemblages studied.

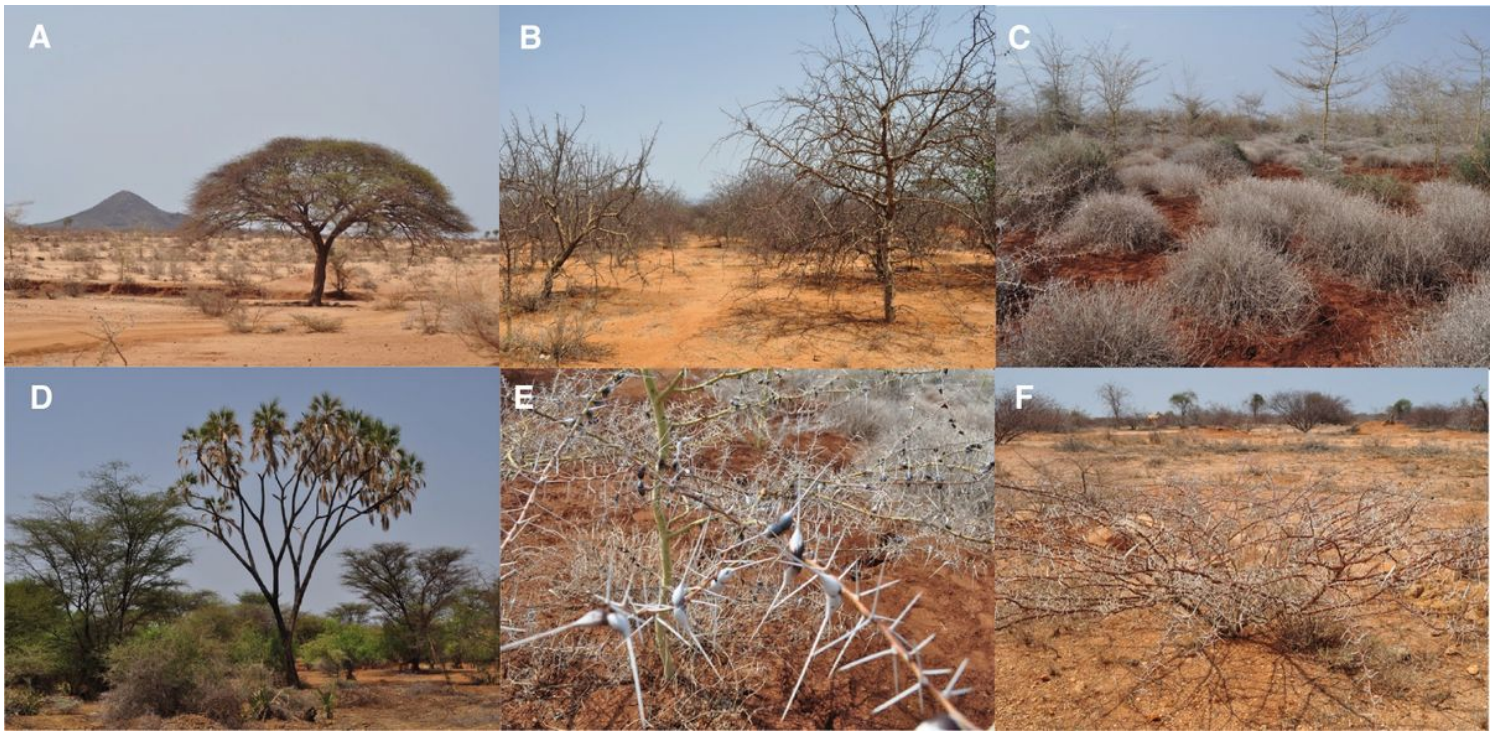

Figure 3

Examples of xerophytic shrubland environments in modern eastern Africa, including typical species (sp.). A) Acacia tortilis B) Commiphora sp. C) Acacia sp. and Duosperma eremophilum. D) Hyphaene compressa, Acacia sp., Salvadora persica, Cyperacea and Lawsonia inermis E) Acacia sp. and Duosperma eremophilum, F) Acacia tortilis (background: Commiphora sp. Capparaceae sp. Tephrosia sp. and Indigofera spinosa).

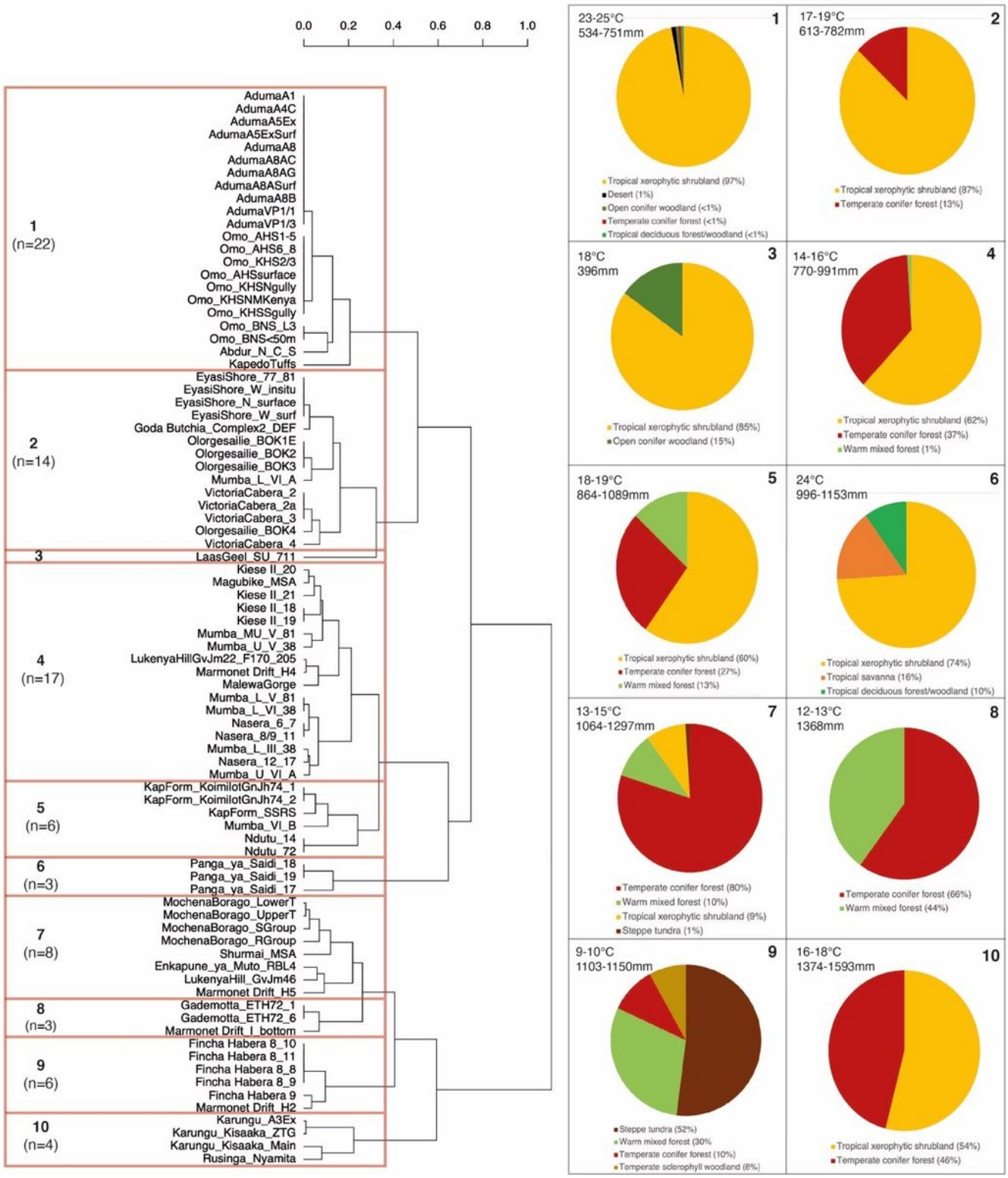

Figure 4

Hierarchical clustering of the assemblages according to mean annual temperature and total annual precipitation. K means clustering identified ten clusters as the optimal division of the dendrogram, which have been highlighted here as well as the range of environmental conditions occupied by each cluster and the percentage of cells within 50km of that biome for all assemblages within that cluster.

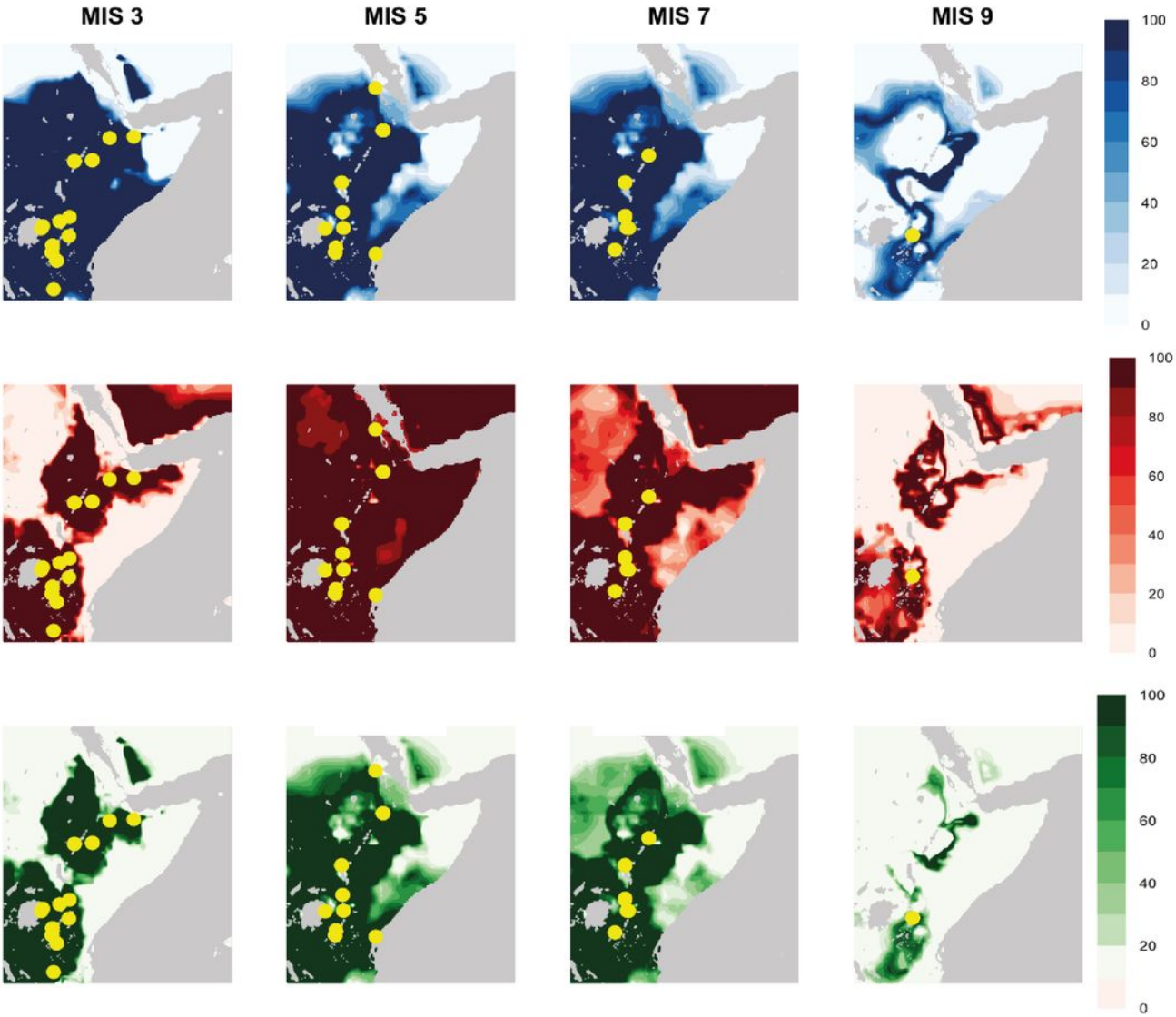

Figure 5

Mean annual temperature (top), total annual precipitation (middle) and combined (bottom) phased models of habitability, demonstrating the percentage of time intervals (1000 years per interval) that remain within the climatic range of the assemblages dated to that Marine Isotope Stage (MIS). The palaeocoastline has been estimated based on the predicted mean sea-level for each MIS.

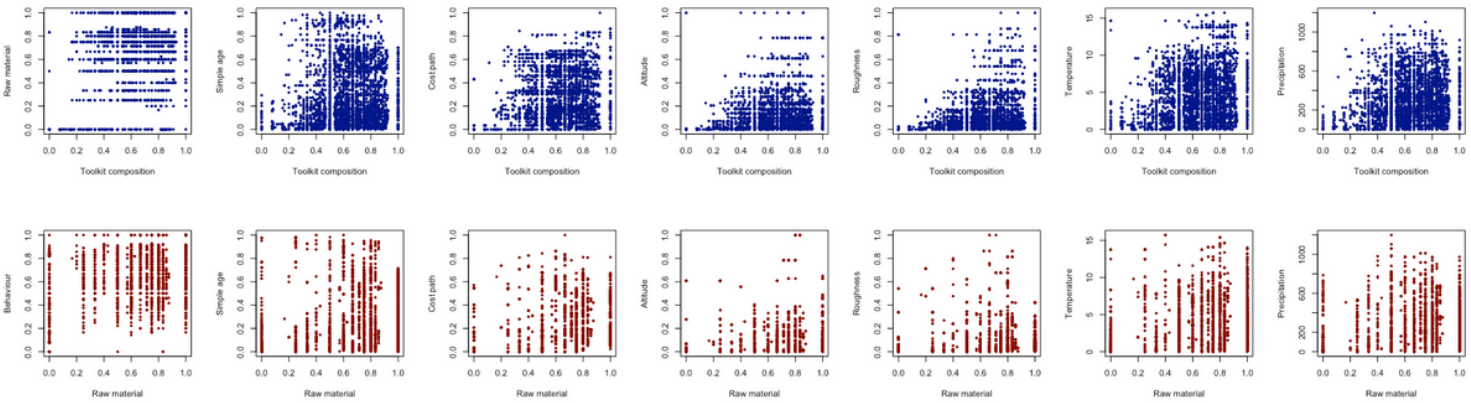

Figure 6

Scatterplots of the Mantel test results (Table 1, Supplementary Table S3-4) between the pairwise distance matrix of toolkit composition (top) and raw material use (bottom) and the other distances matrices excluding the two binary variables, site type and method.

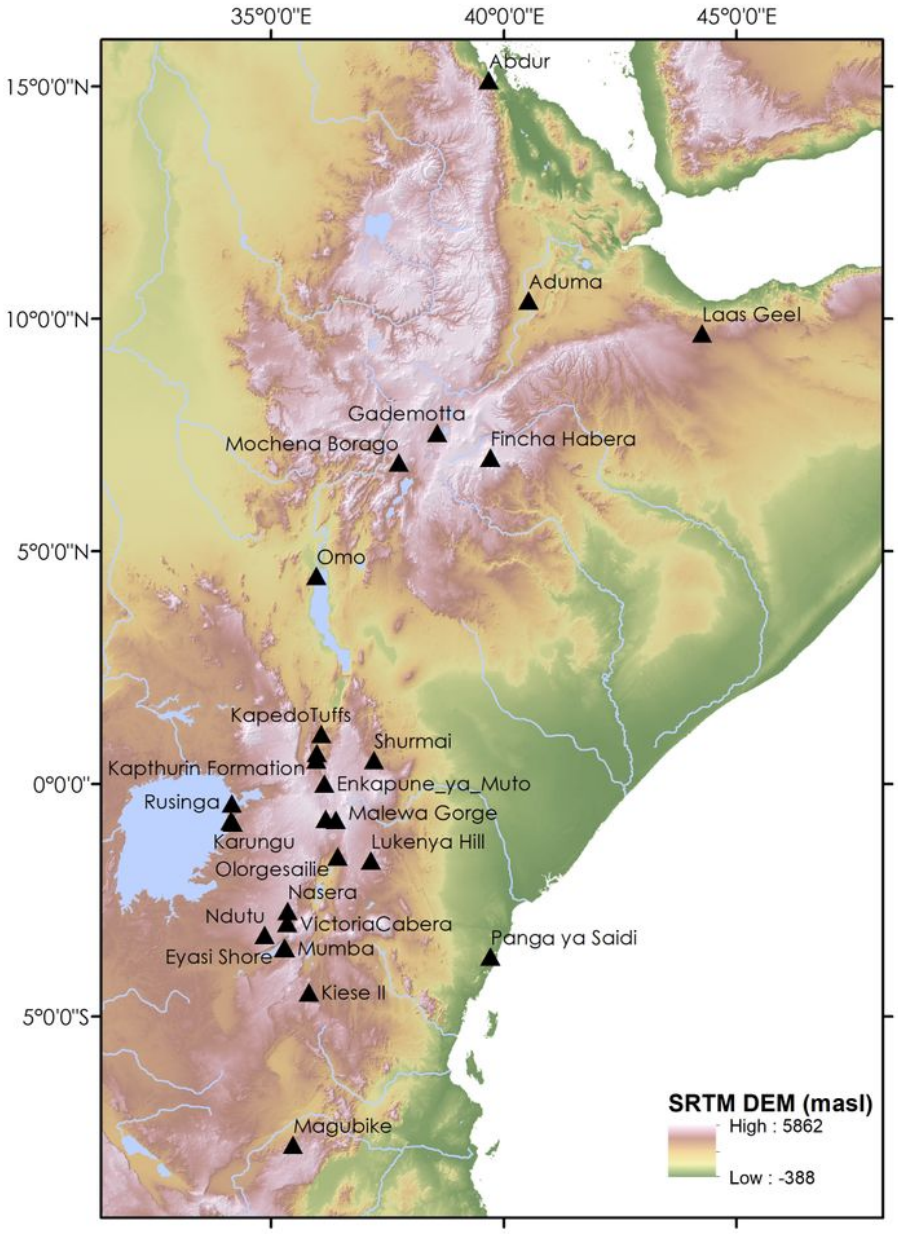

Figure 8

Supplementary Files

This is a list of supplementary files associated with this preprint. Click to download.

- supplementarymaterials1.docx